

The role of DNA in PANI–DNA hybrid: Template and dopant

Xin Li^{a,b}, Meixiang Wan^{a,*}, Xiaoning Li^b, Guoliang Zhao^b

^a Institute of Chemistry, Chinese Academy of Sciences, Beijing 100190, People's Republic of China

^b Beijing Key Laboratory of Clothing Materials R&D and Assessment, School of Materials Science and Engineering, Beijing Institute of Fashion Technology, Beijing 100029, People's Republic of China

ARTICLE INFO

Article history:

Received 25 January 2009

Received in revised form

4 June 2009

Accepted 13 July 2009

Available online 19 July 2009

Keywords:

Polyaniline

DNA

Hybrid

ABSTRACT

We exposed a novel method by using DNA as the dopant as well as template at the same time to prepare PANI–DNA hybrid micro/nanowires with conductivity as high as $\sim 10^{-2} \text{ S cm}^{-1}$. The high conductivity is due to the co-doping function of DNA with HCl produced by FeCl_3 . It is found that the morphology and conductivity of the PANI–DNA hybrids are affected by the $[\text{DNA}]/[\text{AN}]$ ratio due to the co-operation and competition of DNA's dopant and template function, and the role of DNA in PANI–DNA hybrid varies with the changing of $[\text{DNA}]/[\text{AN}]$ ratios.

© 2009 Elsevier Ltd. All rights reserved.

1. Introduction

Bio-molecule templates give new opportunities to construct novel nano-materials with special features [1–3]. Among those bio-templates, deoxyribonucleic acid (DNA) has recently received great attention because its special self-recognition and self-assembly properties offer unique advantages for design and synthesis of multifunctional bio-active molecular complex [4–6]. In addition, micro/nanostructures of conducting polymers, such as polyaniline (PANI) or polypyrrole (PPy), have also drawn great interests due to their unique chemical and physical properties [7–11] including controllable chemical and electrical properties by simply changing the oxidation and proton state, facile and low cost of preparation, and excellent environmental stability. These unique properties lead to the wide applications of conducting polymers in micro/nano-materials [12–14] and devices, such as light-emitting diodes [15,16], transistors [17], chemical and biosensors [18,19], solar cells [20], electrochromic devices [21] and memory devices [22]. It is therefore reasonable to be expecting that combination of the reversible doping/de-doping feature of conducting polymers with molecular-recognition and self-assembly characteristic of DNA [23,24] might expose wide applications in molecular electronic device and quantum functional materials [25]. So far, a series of articles on nanostructured hybrids of conducting polymers with DNA have been reported. For instance, Y.F. Ma and co-workers [26]

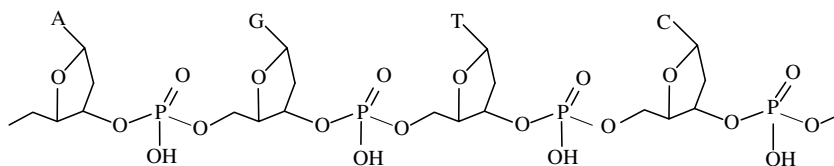
reported a strategy for the fabrication of conducting polymer nanowires on thermally oxidized Si surface by using DNA as the hard-template. Nagarajan et al. [27] used DNA as the hard-template to prepare water-soluble PANI–DNA complexes, in which PANI was wrapped around the DNA and it can reversibly control the secondary structure of DNA from the native form to an over-wound polymorph by simply changing the redox state of PANI. Moreover, a hybrid of poly(*o*-methoxy-aniline) with DNA, which has a needle-like morphology and conductivity of ca. $10^{-7} \text{ S cm}^{-1}$, has been reported by Dawn et al. [24] Except for PANI–DNA complexes, PPy–DNA hybrids have also been reported [28]. As to our best knowledge, DNA in the previous papers mainly was used as the hard-template and the conductivity of the resultant nanostructured hybrid was quite poor [24,26]. Consequently, exploring new function of DNA for enhancing conductivity of the conducting polymer hybrids with DNA is urgently necessary.

As Scheme 1 shows [28], DNA molecule has phosphate groups which can act as the dopant of PANIs due to their proton doping mechanism [7], suggesting that the doping function of DNA might be imposed. Recently, Wan et al. [29–31] reported a simplified template-free method (STFM) to prepare PANI nanotubes with 20–30 nm in diameter and PANI derivatives with hollow microspheres in shape by using FeCl_3 as both oxidant and dopant in the absence of acidic dopant and hard-template. This STFM is the simplest approach to prepare PANI nanostructures at the current time because only aniline monomer and oxidant are required.

Herein, we report a novel approach to prepare self-assembly microwires of PANI–DNA hybrid with conductivity as high as $1.3 \times 10^{-2} \text{ S cm}^{-1}$ by using DNA as dopant as well as hard- and soft-

* Corresponding author. Tel.: +86 10 64288225.

E-mail address: xinli@iccas.ac.cn (M. Wan).



Scheme 1. Molecular structure of DNA.

template. Interestingly, these hybrid microwires are constructed by the nanofibers with about 20–30 nm in diameter. Moreover, the morphology and conductivity of the hybrid are greatly affected by the mass ratio of DNA to aniline. The role of DNA as dopant and template is discussed based on the molecular characterizations, as measured by FTIR and UV–vis spectrum, X-ray photoelectron spectroscopy (XPS), synchronous energy dispersive X-ray (EDX) and X-ray diffraction (XRD), as well as the conductivity measured by a four-probe method.

2. Experimental

2.1. Materials

Deoxyribonucleic acid (DNA) from salmon test was purchased from Sigma Chemical Co., USA (D-1626, type III, sodium salt). All the experiments involving DNA were performed under sterilized conditions. Before each reaction, DNA was firstly dissolved in the water under magnetic stirring to form a homogeneous and transparent aqueous solution. Aniline (A.R., Beijing Mashu Fine Chem. Co.) was distilled under reduced pressure and kept refrigerated under nitrogen prior to use. Other reagents, such as Ferric chloride hexa-hydrate ($\text{FeCl}_3 \cdot 6\text{H}_2\text{O}$, Tianjin Shuangchuan Chem. Reagent Factory), *m*-cresol (Tianjin Wenda Xigui Chemical Plant) and ethanol (Beijing Chemical Plant), were all of A.R. grade and used as received without further treatment. Besides, pH-meter (PHS-W) was used to measure the pH value of the reaction solution.

2.2. Characterization

Field emitting scanning electron microscope (SEM, JSM-6700F) and transmission electron microscope (TEM, JEM-200CX) were used to measure the morphology of DNA, PANI and PANI–DNA. The molecular structure was characterized by FTIR spectra (Perkin-Elmer System), ultraviolet–visible absorption spectrum (SHIMADZU UV-1601PC UV–vis spectrophotometer), X-ray photoelectron spectroscopy (XPS, ESCALab220i-XL), synchronous energy dispersive X-ray (EDX) and X-ray diffraction (XRD, RINT2000 Wide angle goniometer). The conductivity at room temperature was measured by a four-probe method with a Keithley 196 SYSTEM DMM digital multi-meter and an ADVANTEST R6142 programmable DC voltage–current generator as the current source.

2.3. Synthesis procedure

The PANI–DNA hybrid microwires were synthesized by using DNA as the dopant as well as template at the same time in the presence of $\text{FeCl}_3 \cdot 6\text{H}_2\text{O}$ as the oxidant. A typical synthesis procedure is as follows. First, a pre-designed amount (0.2–20 mg) of DNA was dissolved in 10 mL de-ionized water with magnetic stirring at room temperature to form transparent solution (pH = 6.78–6.91). Next, 0.183 mL aniline was added into the mixture and kept stirring for about 30 min at room temperature to form a uniform mixture solution, and then 8 mL $\text{FeCl}_3 \cdot 6\text{H}_2\text{O}$ aqueous solution (1.0 M) was dripped into the mixture for about 40–50 min at 0–5 °C (with

ice–water bath). After about 10 h reaction, the resulted dark-green suspension was filtered and washed with de-ionized water and then ethanol for several times. Finally, the product was dried under vacuum at 60 °C for 12 h to obtain a dark-green powder that was represented by PANI–DNA hybrid. The PANI nanofibers were also synthesized by a similar synthesis procedure in the absence of DNA, which were represented by PANI.

3. Results and discussion

Fig. 1 shows SEM images of PANI and the PANI–DNA hybrids synthesized at different mass ratios of DNA to aniline, which are represented as $[\text{DNA}]/[\text{AN}]$ ratios. As shown in Fig. 1a, the PANI, which was synthesized in the absence of DNA, is fibril morphology in shape with 20–30 nm in diameter and about 200 nm in length that is consistent with the previous results [29]. At a lower $[\text{DNA}]/[\text{AN}]$ ratio (e.g. 0.011), the PANI–DNA is composed of nanofibers with about 30–50 nm in diameter and ~100 nm in length (Fig. 1b), indicating that the morphology of the PANI–DNA is similar to that of the PANI but with a slightly larger diameter and less length. When the $[\text{DNA}]/[\text{AN}]$ ratio is increased to 0.054, although PANI–DNA is still composed of nanofibers with ~20 nm in diameter, however, these nanofibers arrange in a certain way and make up the microwire with ~1 μm in diameter and over 10 μm in length (Fig. 1c and d). When the $[\text{DNA}]/[\text{AN}]$ ratio is further increased to 0.07, interestingly, the resulted PANI–DNA shows a helical microwire in shape with 0.5–0.8 μm in diameter (Fig. 1e and g), which is constructed with helical nanowires with 100–200 nm in diameter observed from SEM image at a higher magnification (see Fig. 1f), similar with the morphology of the solid DNA (Fig. 1h), indicating that DNA plays a role of hard-template inducing the formation of the helical PANI–DNA microwires. As shown in Fig. 1h, the solid DNA is constructed by the helical nanowires with 120–150 nm in diameter, which is much bigger than that of one single strand DNA (~2 nm in diameter) [32,33], suggesting DNA used in this study is composed of a lot of single strand of DNA that can serve as the hard-template forming the helical microwires of PANI–DNA.

In addition, the conductivity of PANI–DNA is also affected by the $[\text{DNA}]/[\text{AN}]$ ratios. As shown in Fig. 2, the conductivity of PANI–DNA increases with the increase of the $[\text{DNA}]/[\text{AN}]$ ratios until it achieves a maximum value at the $[\text{DNA}]/[\text{AN}]$ equal to 0.054, and then followed by decreasing conductivity. The maximum conductivity of the PANI–DNA at the $[\text{DNA}]/[\text{AN}]$ ratio of 0.054 is calculated to be about $1.3 \times 10^{-2} \text{ S cm}^{-1}$, as measured by a four-probe method. This is enhanced by over 70 times compared with the conductivity of the PANI ($0.18 \times 10^{-3} \text{ S cm}^{-1}$), proving that DNA has the doping function to the PANI–DNA.

In order to further understand the role of DNA in PANI–DNA hybrid, the molecular structure of the PANI and as-synthesized PANI–DNA at different $[\text{DNA}]/[\text{AN}]$ ratios dissolved in *m*-cresol was firstly characterized by means of UV–vis spectra. As shown in Fig. 3a, the electronic structures of the PANI–DNA are similar to that of the PANI, which has two bands at 330 nm and 432 nm (assigned as the π – π^* and n – π^* transition respectively) [34] and with a long tail from 800 nm to 1200 nm (assigned as the delocalized polaron

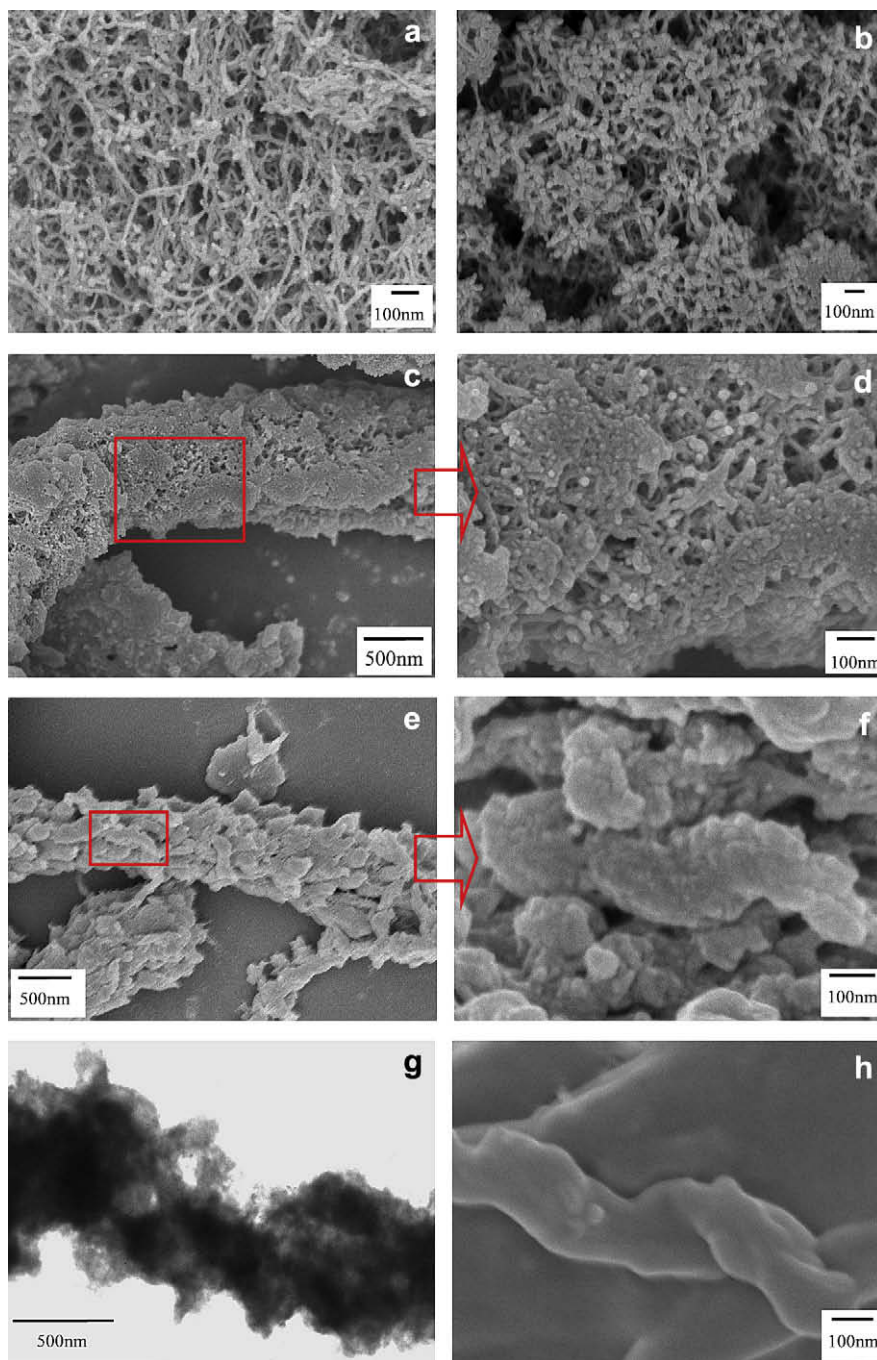


Fig. 1. Morphology of PANI, PANI-DNA hybrid and DNA. (a): SEM images of PANI; (b)–(f): SEM images of PANI-DNA prepared at $[DNA]/[AN] = 0.011, 0.054$ and 0.07 respectively; (g): TEM images of PANI-DNA prepared at $[DNA]/[AN] = 0.07$; (h): SEM image of pure DNA in solid state. Other synthesis conditions: $[FeCl_3]/[AN] = 4:1$, $T = 0-5^\circ C$.

band) [35], indicating that the resulted PANI-DNA hybrids belong to the conducting state of PANI. Moreover, the polymeric chain structure of PANI-DNA was also similar to the PANI, as measured by FTIR. As shown in Fig. 3b, all characteristic bands of PANI [36–38], such as the C=C stretching deformation of the quinoid at 1562 cm^{-1} and benzenoid rings at 1494 cm^{-1} , the C–N stretching of the secondary aromatic amine at 1296 cm^{-1} , the aromatic C–H in plane bending at 1128 cm^{-1} , and the out-of-plane deformation of C–H in the 1,4-disubstituted benzene ring at 802 cm^{-1} and 507 cm^{-1} are all quite distinct in PANI-DNA. Besides, the bands at 3440 cm^{-1} and 3221 cm^{-1} , attributed to the N–H and =NH stretching modes respectively, are also observed. However, the

bands at 2924 cm^{-1} and 2854 cm^{-1} assigned to the vibration of P–OH of phosphate group in the DNA chain, and two bands at 1730 cm^{-1} and 675 cm^{-1} attributed to the stretching vibration of C=O double band in DNA base pairs [6,39] and asymmetric stretching of P–O–C respectively [40] are only appeared from the PANI-DNA prepared at relatively higher $[DNA]/[AN]$ ratios (e.g. $[DNA]/[AN]$ at 0.054 and 0.07 , respectively), and the peaks in Fig. 3b(4) ($[DNA]/[AN] = 0.07$) are more distinct than in Fig. 3b(3) ($[DNA]/[AN] = 0.054$). In spite of these, the peak at 1375 cm^{-1} assigned as the C–N stretching vibration of *trans* isomer of PANI [41] disappears for PANI-DNA prepared at $[DNA]/[AN] = 0.07$ as shown in Fig. 3b(4), this phenomenon combines with other petty

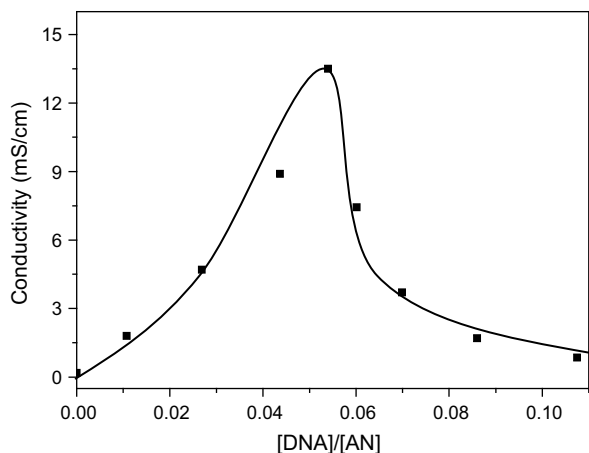
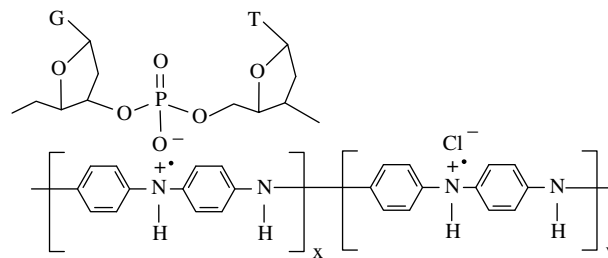


Fig. 2. Room-temperature conductivity of the PANI-DNA hybrid as a function of [DNA]/[AN] ratios. Other synthesis conditions: $[\text{FeCl}_3]/[\text{AN}] = 4:1$, $0\text{--}5^\circ\text{C}$.

spectrum shifts and variation in FTIR indicating that DNA has influenced the PANI-DNA molecular backbone especially under a higher content. On all accounts, the FTIR results clearly demonstrate that DNA has been incorporated into the PANI-DNA hybrid, and the proportion of DNA in the PANI-DNA hybrid increases with the increase of [DNA]/[AN] ratio. However, by now, it still cannot be sure that if DNA is chemically combined with PANI or not, and how they are combined together.

As above-mentioned, FeCl_3 can be served as oxidant and dopant at the same time due to the produced HCl by its hydrolyzation, which is a common dopant of PANI [42]. According to general acid-doping mechanism of PANI, on the other hand, via its PO_4^{3-} group, DNA can also act as the dopant for PANI. Consequently, PANI-DNA is expected to be doped by DNA and HCl as co-dopant. Scheme 2 gives the assumed PANI-DNA hybrid formula co-doped by DNA and Cl^- , where x and y representing the doping degree induced by DNA and Cl^- respectively, which can be determined by the content ratio of P and Cl elements usually. In order to prove the above proposal, the XPS spectra of the PANI-DNA and PANI are measured, and the results are given in Fig. 4 and the supporting information Fig. S2. It can be seen from Fig. 4a that the band of P2p appears at 133.9 eV and is only observed for PANI-DNA hybrid, which is the characteristic of (PO_4^{3-}) group in DNA, indicating that (PO_4^{3-}) acts as the counter anion in PANI-DNA hybrid. At the same time, a band of Cl2p at 197.1 eV (Fig. 4b) as well as a band of Fe2p at 712.2 eV (supporting information Fig. S2) is also observed for both



Scheme 2. The assumed PANI-DNA hybrid formula co-doped by DNA and Cl^- (x , y representing different doping degrees of DNA and Cl^-).

PANI-DNA hybrid and PANI, showing FeCl_3 acting as the co-dopant. Moreover, three deconvoluted peaks of N1s spectra appearing around 398 eV, 399 eV and 401 eV, are found for both PANI-DNA and PANI (Fig. 4c and d), which belong to characteristic components of quinonoid imine ($=\text{N}-$), benzenoid amine ($-\text{NH}-$) and positively charged nitrogen ($-\text{N}^+-$) [43] respectively, accordingly indicating both of them are in doping state. Comparing the ($-\text{N}^+-$) band energy of PANI-DNA and PANI, it can be found that the former is lower (401.2 eV) than that of the latter (401.7 eV), which is the result of the increased electron cloud density arising from the formation of new bond ($-\text{O}^+-\text{NH}-$) induced by the doping function of PO_4^{3-} , proving that PO_4^{3-} is chemically combined with the PANI backbone in the usual manner of dopant.

Besides, EDX results of the PANI-DNA and PANI (see supporting information Fig. S1) give further supports on the above proposal. Similarly, the detection of Cl and Fe elements from both PANI-DNA and PANI, indicates that FeCl_3 serves as oxidant and dopant at the same time, that is also consistent with our previous results [42]. Besides, Cl and P elements are also detected in the PANI-DNA, suggesting that the PANI-DNA is doped by DNA and HCl as the co-dopant. Thereby, the total doping degree in the PANI-DNA is assigned as $(\text{Cl} + \text{P})/\text{N}$ and calculated to be 0.499–0.545 except for 0.38 of the sample prepared at [DNA]/[AN] = 0.07 (see Table 1), further indicating that PANI-DNA is identical to the emeraldine salt form of PANI, whose doping degree is general at around 0.5. The lower doping degree of 0.38 for the sample prepared at [DNA]/[AN] = 0.07 may be attributed to two reasons: one is DNA's hard-template function at a high [DNA]/[AN] ratio, the other is the steric hindrance of the excessive DNA macromolecules. Interestingly, it is noted that the contribution of HCl and DNA to the total doping degree is also affected by the [DNA]/[AN] ratios. For instance, the doping degree by HCl (i.e. y value in Scheme 2) decreases with the increase of [DNA]/[AN] ratios, while the doping degree by DNA (i.e.

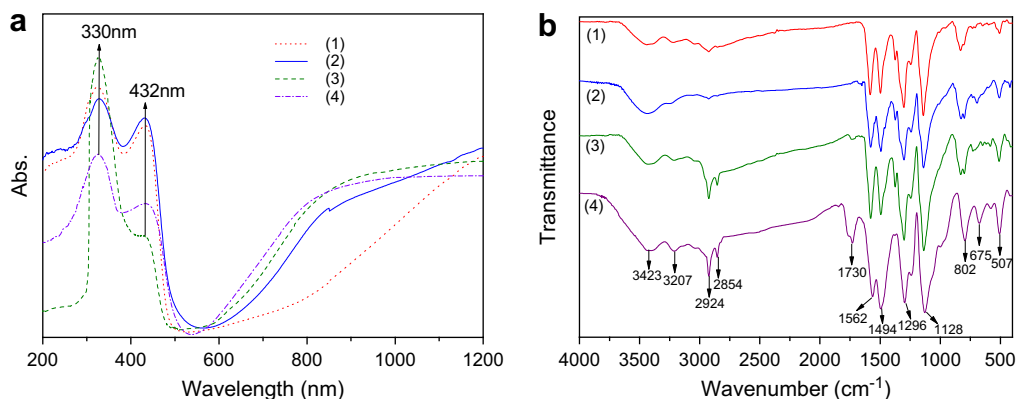


Fig. 3. UV-vis (a) and FTIR (b) spectra of PANI and PANI-DNA. (1): PANI; (2)–(4): PANI-DNA prepared at [DNA]/[AN] = 0.011, 0.054 and 0.070, respectively. Other preparation conditions: $[\text{FeCl}_3]/[\text{AN}] = 4:1$, $T = 0\text{--}5^\circ\text{C}$, and the samples are dissolved in *m*-cresol for UV-vis spectra test.

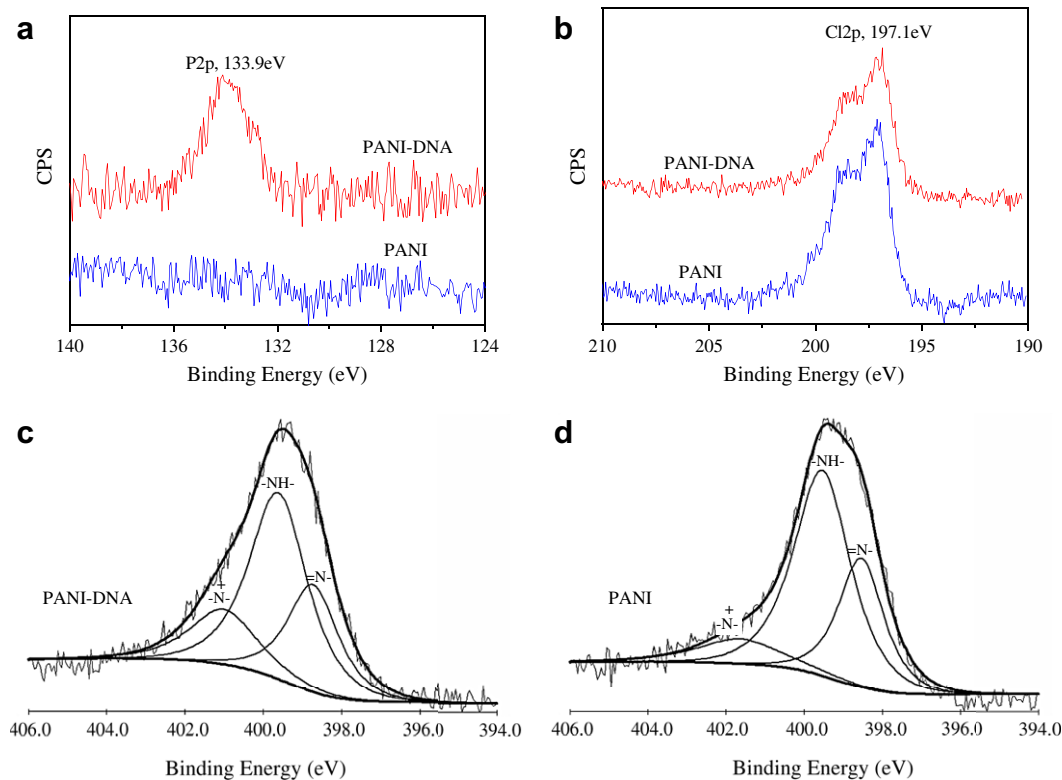


Fig. 4. XPS spectra of PANI and nanofiber-constructed helical PANI–DNA microwires prepared at $[DNA]/[AN] = 0.054$. (a): Cl2p, (b): P2p, (c) and (d): N1s of PANI–DNA and PANI respectively.

x value in Scheme 2) increases with the increase of the $[DNA]/[AN]$ ratios before it reaches to the critical value, and then decreases with the increase of $[DNA]/[AN]$ ratio (see Table 1). Based on above-results, it is reasonable to suggest that, at a lower $[DNA]/[AN]$ ratio, DNA mainly acts as the co-dopant for PANI–DNA, resulting in the increasing conductivity with the increase of $[DNA]/[AN]$ ratios. At a higher $[DNA]/[AN]$ ratios, on the other hand, DNA is mainly served as the hard-template to form the helical microwires, in which the hard-template function as well as the steric effect of insulated DNA results in the decreasing conductivity of PANI–DNA with the increase of the $[DNA]/[AN]$ ratios. In brief, the above discussion can interpret why the conductivity is decreased and the helical morphology is observed at a higher $[DNA]/[AN]$ ratios as shown in Figs. 1 and 2, respectively.

The crystalline of pure DNA, PANI and PANI–DNA was also measured by XRD. As shown in Fig. 5, the XRD spectra of the PANI–DNA prepared at lower $[DNA]/[AN]$ ratio (e.g. 0.011 and 0.054) have some sharp peaks at $2\theta = 9.5^\circ(001)$, $15.1^\circ(011)$, $20.4^\circ(020)$ and $25^\circ(200)$ and a weak peak at $26.5^\circ(121)$, which are in the monoclinic space group $P2_1$ [44], showing higher crystalline and similar to that of PANI. However, the PANI–DNA prepared at a higher $[DNA]/[AN]$ ratio (e.g. 0.07) only has one broad peak centred at

$2\theta = 23.6^\circ$, which is similar to that of pure DNA and shows amorphous. All above-described results suggest that DNA is served as template and dopant at the same time that differs from the previous results, where DNA only plays a role of hard-template.

Generally, DNA is mainly used as the hard-template to prepare hybrids or nanostructures of conducting polymers with DNA. According to our previous results [30,45], when DNA is used as the dopant, it is expected to be functioning as the soft-template in the self-assembly of PANI nanofibers or nanotubes. These results suggest that DNA is able to play a role of soft- and hard-template at the same time in the formation of the PANI–DNA hybrids. However,

Table 1
Influence of the $[DNA]/[AN]$ ratios on the doping degree by HCl and DNA calculated from EDX analysis results.

Samples	$[DNA]/[AN]$ [g/g]	Cl/N	P/N	(Cl + P)/N
PANI	0	0.545	0	0.545
PANI–DNA	0.027	0.447	0.052	0.499
PANI–DNA	0.054	0.322	0.202	0.524
PANI–DNA	0.070	0.281	0.099	0.380

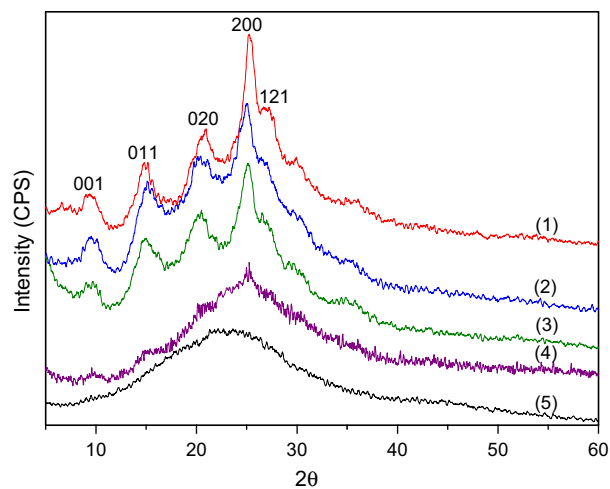


Fig. 5. XRD spectra of PANI and PANI–DNA. (1): PANI; (2)–(4): PANI–DNA prepared at $[DNA]/[AN] = 0.011$, 0.054 and 0.070 , respectively; (5): pure DNA in solid state. Other synthesis conditions: $[FeCl_3]/[AN] = 4:1$, $0-5^\circ C$.

the competition between the soft-template and hard-template by DNA is related to the [DNA]/[AN] ratios that results in the morphology variation of PANI–DNA with the [DNA]/[AN] ratios. At a lower [DNA]/[AN] ratio, soft-template by DNA is dominated, resulting in the formation of PANI–DNA nanofibers, which is similar to that of the PANI. At a higher [DNA]/[AN] ratio, on the other hand, co-operation of soft- and hard-template by DNA results in helical PANI–DNA microwires constructed with nanofibers or helical nanowires. In other words, the helical PANI–DNA including microwires or nanowires is induced by DNA functioned as the hard-template, while the PANI–DNA nanofibers are self-assembled by DNA functioned as the soft-template.

4. Conclusion

In summary, we expose a novel method by using DNA as the dopant as well as hard- and soft-template to prepare PANI–DNA hybrid micro/nanowires with conductivity as high as $\sim 10^{-2} \text{ S cm}^{-1}$. Both the morphology and conductivity of the PANI–DNA hybrids are affected by the [DNA]/[AN] ratios. It is proved that the change of conductivity with the [DNA]/[AN] ratios results from the competition of DNA and HCl as the co-dopant. On the other hand, the co-operation and competition of DAN as the soft- and hard-template result in the morphology variation of the PANI–DNA with the [DNA]/[AN] ratios.

Acknowledgements

This project was supported by The National Nature Sciences Foundation of China (No. 50533030) and The Beijing Nova Programme (2007B010), and we would like to thank Prof. Wei Yen at the Centre for Advanced Polymers and Materials Chemistry, Department of Chemistry, Drexel University, Philadelphia, USA for providing DNA samples.

References

- [1] Gasparac R, Kohli P, Mota MO, Trofin L, Martin CR. *Nano Lett* 2004;4(3):513.
- [2] Ma N, Dooley CJ, Kelley SO. *J Am Chem Soc* 2006;128(39):12598.
- [3] Krummel AT, Zanni MT. *J Phys Chem B* 2008;112(5):1336.
- [4] Masanori Y, Hirofumi A. *Polymer* 2008;49(21):4658.
- [5] Ramanathan K, Bangar MA, Yun M, Chen W, Myung NV, Mulchandani A. *J Am Chem Soc* 2005;127(2):496.
- [6] Nayak S, Andrew LL. *Angew Chem Int Ed* 2005;44:7686.
- [7] MacDiarmid AG. *Angew Chem Int Ed* 2001;40:2581.
- [8] Chen XH, Chen GM, Ma YM, Li XH, Jiang L, Wang FS. *J. Nanosci Nanotechnol* 2006;6:783.
- [9] Li Y, Shi GQ. *J Phys Chem B* 2005;109(50):23787.
- [10] Lawrence Jr TS, Wei Y, Jansen SA. *J Phys Chem A* 2000;104(48):11371.
- [11] Luo J, Wang XH, Li J, Zhao XJ, Wang FS. *Polymer* 2007;48(15):4368.
- [12] Qin LD, Park S, Huang L, Mirkin CA. *Science* 2005;309:113.
- [13] Lipomi DJ, Chiechi RC, Dickey MD, Whitesides GM. *Nano Lett* 2008;8(7):2100.
- [14] Berdichevsky Y, Lo YH. *Adv Mater* 2006;18:122.
- [15] Müller CD, Falcou A, Reckefuss N, Rojahn M, Wiederhirn V, Rudati P, et al. *Nature* 2003;421:829.
- [16] Ma W, Iyer PK, Gong X, Liu B, Moses D, Bazan GC, et al. *Adv Mater* 2005;7(3):274.
- [17] Jeffrey AM, Daniel CF. *J Polym Sci Part B Polym Phys* 2003;41(21):2674.
- [18] Ayad MM, Salahuddin NA, Abou-Seif AK, Alghaysh MO. *Polym Adv Technol* 2008;19(8):1142.
- [19] Aoife M, Orawan N, Anthony JK, Simon EM, Malcolm RS, Gordon GM. *Electroanalysis* 2005;17:423.
- [20] Xia J, Masaki N, Lira-Cantu M, Kim Y, Jiang K, Yanagida S. *J Am Chem Soc* 2008;130(4):1258.
- [21] Yang CH, Huang LR, Chih YK, Chung SL. *J Phys Chem C* 2007;111:3786.
- [22] Tseng RJ, Huang JX, Ouyang JY, Kaner RB, Yang Y. *Nano Lett* 2005;5(6):1077.
- [23] Wei Y, Yang Y, Yeh JM. *Chem Mater* 1996;8(11):2659.
- [24] Dawn A, Nandi AK. *Macromol Biosci* 2005;5:441.
- [25] Taira S, Yokoyama K. *Biotechnol Bioeng* 2005;89(7):835.
- [26] Ma YF, Zhang JM, Zhang GJ, He HX. *J Am Chem Soc* 2004;126:7097.
- [27] Nagarajan R, Liu W, Kumar J, Tripathy SK, Bruno FF, Samuelson LA. *Macromolecules* 2001;34:3921.
- [28] Komarova E, Aldissi M, Bogomolova A. *Biosens Bioelectron* 2005;21:182.
- [29] Ding HJ, Wan MX, Wei Y. *Adv Mater* 2007;19:465.
- [30] Ding HJ, Shen JY, Wan MX, Chen ZJ. *Macromol Chem Phys* 2008;209:864.
- [31] He HY, Zhu Y, Li X, Wang QB, Wan MX, Jiang L. *Acta Polym Sin* 2008;12:1172.
- [32] Alain P, Bernard T, Jean S, Gilbert W. *Electrophoresis* 1998;19:1548.
- [33] Sung CH, Lowenhaupt K, Alexander R, Kim YG, Kyeong KK. *Nature* 2005;437:1183.
- [34] Wei Y, Tang X, Sun Y, Focke WW. *J Polym Sci Part A Polym Chem* 1989;27(7):2385.
- [35] Huang K, Wan MX. *Chem Mater* 2002;14:3486.
- [36] Wei Y, Ramakrishnan H, Sandeep AP. *Macromolecules* 1990;23(3):758.
- [37] Zhang LJ, Wan MX. *Adv Funct Mater* 2003;13(10):815.
- [38] Wei ZX, Wan MX. *Adv Mater* 2002;14(18):1314.
- [39] Lokshin NA, Sergeev VG, Zezin AB, Golubev VB, Levon K, Kabanov VA. *Langmuir* 2003;19:7564.
- [40] Thompson LA, Kowalik J, Josowicz M, Janata J. *J Am Chem Soc* 2003;125:324.
- [41] Kang ET, Neoh KG, Tan KL. *Prog Polym Sci* 1998;23:277.
- [42] Ding HJ, Zhu CJ, Zhou ZM, Wan MX. *Acta Polym Sin* 2007;5:462.
- [43] Kim BJ, Oh SG, Han MG, In SS. *Langmuir* 2000;16:5841.
- [44] Stejskal J, Riede A, Hlavatá D, Prokes J, Helmstedt M, Holler P. *Synth Met* 1998;96:55.
- [45] Wei ZX, Zhang ZM, Wan MX. *Langmuir* 2002;18:917.